Clinical Biomechanics 42 (2017) 25–30

Contents lists available at ScienceDirect

Clinical Biomechanics

journal homepage: www.elsevier.com/locate/clinbiomech

Subject-specific finite element analysis of the carpal tunnel cross-sectional to examine tunnel area changes in response to carpal arch loading

Piyush Walia [a,c], Ahmet Erdemir [b,c], Zong-Ming Li [a,c,d,e,*]

[a] Hand Research Laboratory, Cleveland Clinic, Cleveland, OH, United States
[b] Computational Biomodeling (CoBi) Core, Cleveland Clinic, Cleveland, OH, United States
[c] Department of Biomedical Engineering, Cleveland Clinic, Cleveland, OH, United States
[d] Department of Orthopaedic Surgery, Cleveland Clinic, Cleveland, OH, United States
[e] Department of Physical Medicine and Rehabilitation, Cleveland Clinic, Cleveland, OH, United States

ARTICLE INFO

Article history:
Received 26 July 2016
Accepted 3 January 2017

Keywords:
Carpal tunnel
Cross-sectional area
Mechanics

ABSTRACT

Background: Manipulating the carpal arch width (i.e. distance between hamate and trapezium bones) has been suggested as a means to increase carpal tunnel cross-sectional area and alleviate median nerve compression. The purpose of this study was to develop a finite element model of the carpal tunnel and to determine an optimal force direction to maximize area.

Methods: A planar geometric model of carpal bones at hamate level was reconstructed from MRI with inter-carpal joint spaces filled with a linear elastic surrogate tissue. Experimental data with discrete carpal tunnel pressures (50, 100, 150, and 200 mm Hg) and corresponding carpal bone movements were used to obtain material property of surrogate tissue by inverse finite element analysis. The resulting model was used to simulate changes of carpal arch widths and areas with directional variations of a unit force applied at the hook of hamate.

Findings: Inverse finite element model predicted the experimental area data within 1.5% error. Simulation of force applications showed that carpal arch width and area were dependent on the direction of force application, and minimal arch width and maximal area occurred at 138° (i.e. volar-radial direction) with respect to the hamate-to-trapezium axis. At this force direction, the width changed to 24.4 mm from its initial 25.1 mm (3% decrease), and the area changed to 301.6 mm^2 from 290.3 mm^2 (4% increase).

Interpretation: The findings of the current study guide biomechanical manipulation to gain tunnel area increase, potentially helping reduce carpal tunnel pressure and relieve symptoms of compression median neuropathy.

1. Introduction

The carpal tunnel is a fibro-osseous structure comprised of the transverse carpal ligament (TCL) at the volar side and the carpal bones at the dorsal, radial, and ulnar sides. The tunnel has an elliptical cross section extending approximately 20 mm in the proximal-distal direction (Cobb et al., 1993; Gabra et al., 2015; Pacek et al., 2010). The nine flexor tendons and median nerve pass through the confined carpal tunnel, making the nerve prone to compression neuropathy, i.e. carpal tunnel syndrome. While surgical treatment of carpal tunnel syndrome may effectively relieve symptoms, the invasive approach results in a number of complications (e.g. scar tissue, pillar pain, and weakness), making non-surgical alternatives desirable.

The biomechanical properties of the carpal tunnel have been investigated with respect to the carpal arch width (CAW). It has been shown that the carpal tunnel has a decreased CAW during wrist flexion and extension in comparison to the neutral wrist position (Garcia-Elias et al., 1992) and an increased CAW after carpal tunnel release surgery (Garcia-Elias et al., 1992; Gartsman et al., 1986). This CAW change is attributable to the mobility of carpal bones which is guided by bone/cartilage configuration and inter-carpal ligaments (Gabra et al., 2012; Xiu et al., 2010). Attempts to widen (Sucher et al., 2005) or narrow (Li et al., 2013; Marquardt et al., 2015; Marquardt et al., 2016) the CAW have been made to alter the carpal tunnel morphological structure as a means to increase the carpal tunnel cross-sectional area (CSA) for median nerve decompression. Widening the CAW can be limited due to the mechanical constraint imposed by the thick band of the transverse carpal ligament. Narrowing of the CAW has been examined by applying forces to the carpal bones in cadaveric hands (Gabra and Li, 2016) and to the radio-ulnar aspects of the wrist in human subjects (Marquardt et al., 2015; Marquardt et al., 2016). Decreasing the CAW at the distal

* Corresponding author at: Cleveland Clinic, 9500 Euclid Avenue, ND20, Cleveland, OH 44195, USA.
E-mail address: liz4@ccf.org (Z.-M. Li).

http://dx.doi.org/10.1016/j.clinbiomech.2017.01.004
0268-0033/

row was demonstrated to increase the volar arch area of the carpal tunnel (Fig. 1), i.e., the area formed by the TCL divided by a reference line from the ridge of the trapezium and hook of the hamate (Li et al., 2009; Li et al., 2011; Li et al., 2013; Marquardt et al., 2015; Marquardt et al., 2016). However, previous studies were limited to the examination of effects of CAW on volar area without the inclusion of the dorsal arch area formed by carpal bones. In addition, the forces applied to the carpal tunnel in previous studies were prescribed along the CAW, and the optimal direction of force application to achieve maximum volar area increase remains unknown, as does the associated total changes in the carpal tunnel area.

Computational modeling is an effective tool to perform parametric analysis of multiple factors that might be challenging in an experimental study. Finite element (FE) representations, representative of patient-specific anatomy, have been utilized to investigate mechanics of different tissues (Martin et al., 2015; Sun et al., 2015). Specific to the wrist, FE analysis has been used to investigate the load transmission through the carpal bones (Carrigan et al., 2003; Gislason et al., 2009), the effects of pathological conditions on wrist joint (Bajuri et al., 2012), wrist mechanics in response to tendon loading (Majors and Wayne, 2011), and changes in carpal load transmission associated with carpal tunnel release (Guo et al., 2009). FE modeling was also used to analyze stress of the carpal tunnel contents and showed that median nerve compression is attributable to structural contact force rather than fluid pressure (Ko and Brown, 2007; Mouzakis et al., 2014). The FE model of the carpal tunnel presented in the current study permits the exploration of different force conditions applied between the trapezium and hamate bone to evaluate the change in CSA using individualized model. This computational approach allows for virtual testing of models with subject-specific bone geometries, where the influence of any force direction can be evaluated to determine desired outcome parameter, e.g. carpal tunnel area. Nonetheless, a comprehensive understanding of the specimen-specific biomechanics of carpal tunnel morphology depends not only on individualized anatomy but also specimen-specific material properties of tissue representations, which in turn dictate the emergent response of the CAW and carpal tunnel CSA changes when subjected to an intervention.

The overall goal of this study was to develop a simplified, specimen-specific model of the wrist to evaluate the role of varying force direction application between the hamate and trapezium bone on CAW and CSA of the distal carpal tunnel. The distal region of the carpal tunnel was selected for this study because it is the narrowest region in the carpal tunnel (Cobb et al., 1993). The first aim was to establish the FE model by determining the individualized material properties of tissue representations using previously collected pressure and bone kinematics data (Li et al., 2011). It was hypothesized that the individualized FE model would agree with the experimental data from the same specimen within 5% error in CSA correspondence. The second aim was to conduct clinically relevant simulations of mechanical manipulation of CAW and

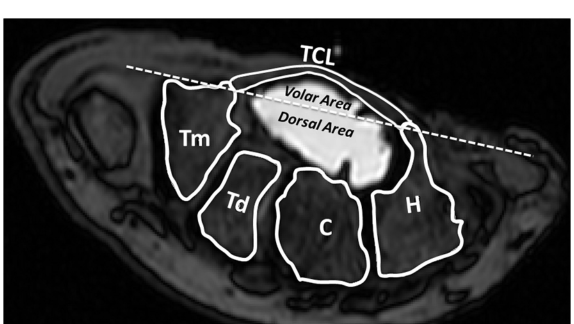

Fig. 1. Segmentation of the transverse carpal ligament (TCL) and four distal carpal bones from a magnetic resonance image. The dashed line along the CAW divides the total carpal tunnel into volar and dorsal areas. Tm = trapezium, Td = trapezoid, C = capitate, H = hamate, and TCL = transverse carpal ligament.

carpal tunnel area. Specifically, the optimal force direction, i.e., the force direction which maximized carpal tunnel CSA, was determined by quantifying CSA change associated with varying force directions. It was hypothesized that the amount of CSA change would be dependent on the orientation of the applied force, increasing area with inward force and decreasing area with outward force.

2. Methods

The overall strategy to achieve the goals of the study relied on finite element analysis of the distal carpal tunnel to predict the CAW and carpal tunnel CSA under various loading and boundary conditions. Technical steps included the model development, inverse finite element analysis to obtain specimen-specific tissue properties, and clinically relevant simulations to understand the influence of the external force orientation on the CAW and carpal tunnel CSA. Data from a previously conducted experimentation on pressure-area relationship were utilized for development of the model and for inverse finite element analysis. All simulations were conducted using Abaqus CAE (v6.10, Simulia, Rhode Island, USA).

The specimen used for finite element analysis was a left wrist from a 42 years old female donor. Experimental data were collected in a previous study (Li et al., 2011). The specimen was a representative closer to the mean CAW and CSA of all. In the experiment, a balloon was inserted in the tunnel and pressurized at 50, 100, 150, and 200 mm Hg. For each pressure level, including the unloaded state of 0 mm Hg, magnetic resonance images (MRI) of the carpal tunnel cross section were collected. An extremity MRI system with a strength of 1 Tesla (OrthOne, ONI Medical Systems Inc., MA, USA) was used to obtain carpal tunnel cross sections with a slice thickness of 1 mm and resolution of 3.4 pixels per mm. Axial images were obtained by 3D gradient echo (TR = 30 ms, TE = 8.9 ms, flip angle = 358) with a 150 × 150 mm^2 field of view and 260 × 192 matrix. The protocol was adjusted such that (1) the axial imaging plane was obliquely oriented at 13° so that the slice plane was perpendicular to the dorsal side of the carpal tunnel (the sagittal scout images were used to determine the angle of oblique orientation for specimen); and (2) the number of image slices was set 32 for the specimen based on the measured length of the carpal tunnel during dissection. The data were processed to characterize the movement of the carpal bones relative to the trapezium as a function of balloon pressure. The coordinates of two points on each bone were extracted for the modeling purpose.

A two-dimensional plane strain model of the distal carpal tunnel cross section with a unit thickness was developed and utilized for this study. The cross-sectional MRI for the unloaded state (0 mm Hg) at the level of the hook of the hamate was used to define a reference geometrical configuration of the transverse carpal ligament and carpal bones (the trapezium, trapezoid, capitate, and hamate; Fig. 1). Manual segmentation of the bones and ligament was performed using the polygon selection tool in ImageJ (v1.43, National Institutes of Health, USA). The mechanics of bones are dictated by the combined mechanical response of cartilage and the surrounding intercarpal ligaments. In the model, the cartilage and the intercarpal ligaments were not modeled explicitly. Instead, the joint spaces between bones were filled with a surrogate tissue to represent the combined mechanical constraints of these structures, both in tension and compression. Then the geometries of the bones and surrogate tissue were reconstructed using Rhinoceros software (v.5, Robert McNeel & Associates, USA) (Fig. 2) and were imported into Abaqus CAE to create the FE model. The geometrical components were meshed with element type C3D8R; the mesh density was updated by conducting preliminary simulations to ensure that CAW predictions did not change by more than 0.5% with increase in the mesh size. The carpal bones were modeled as a co-rotational linear material with Young's modulus and Poisson's ratio of 10,000 MPa and 0.33, respectively (Guo et al., 2009). The surrogate tissue was modeled as a co-rotational linear material with unknown material properties